Preparation of Hybrid β-chitosan – Squid Pen Protein Hydrogel Beads by Ionic Liquid Regeneration for Adsorption of Copper (II) and Zinc (II) from Wastewater †

Liyan Moralez, Pedro Nakasu, and Jason Hallett**
Department of Chemical Engineering, Imperial College London, South Kensington, SW7-2AZ, London U.K.
Email: pedronakasu@gmail.com, j.hallett@imperial.ac.uk

Abstract: This study explores the use of squid pen protein to enhance the mechanical properties, chemical stability, and heavy metal ion (Cu^{2+} and Zn^{2+}) affinity of β-chitosan. 1-Butyl-3-methylimidazilium acetate ([BMIM][OAc]) was used to functionalize β-chitosan and prepare hydrogel beads with improved structural integrity and batch uniformity. However, initial experiments noted a reduction in adsorption capacity as the squid pen protein content increased, with Cu^{2+} and Zn^{2+} adsorption being particularly inhibited at lower pH levels due to protonation. Subsequent batch adsorption studies identified optimal conditions for Cu^{2+} and Zn^{2+} uptake and revealed that adsorption followed pseudo-second-order kinetics, indicating chemisorption. The equilibrium isotherms corresponded with the Langmuir model, suggesting monolayer coverage with maximum adsorption capacities of 70.2 mg g^{-1} for Cu^{2+} and 24.0 mg g^{-1} for Zn^{2+}. The potential of squid pen protein as an economical filler for β-chitosan-based adsorbents was validated alongside the efficiency of using [BMIM][OAc] for the non-toxic functionalization of β-chitosan. Support of green chemistry principles was evidenced by a high atom economy and low environmental impact, indicating a sustainable method for preparing effective biosorbents.

Introduction

Heavy metal ions are a significant class of pollutants.[1] Incidents of carcinogenic, mutagenic, and neurotoxic effects on humans have been attributed to certain species.[2] The danger posed by heavy metal ions is exemplified by their potency at innocuous concentrations, high mobility and longevity in organisms due to bioaccumulation.[3] Heavy metals of high priority include copper (Cu^{2+}), cadmium (Cd^{2+}) and zinc (Zn^{2+}).[1]

Adsorption is a promising strategy for the cost-effective and energy-efficient treatment of dilute effluents. Minimum waste is produced owing to regeneration and recycling of adsorbent.[4] However, conventional carbon- and mineral-based adsorbents are limited by complex synthesis methods and susceptibility to severe loss of efficiency after just a few regeneration cycles, respectively.[5] Moreover, traditional powder adsorbents remain infeasible for commercial adoption due to the economic and time constraints of post-treatment separation and recovery, which often involve precipitation, centrifugation or filtration.[6]

The poor economic robustness of traditional adsorbents has invigorated interest in cost-effective alternatives, particularly biosorbents. Chitosan, the N-deacetylated derivative of chitin, is promising due to its biodegradability, biocompatibility, cost-effectiveness and high capacity for heavy metal ion uptake.[3, 7] Specifically, β-chitosan, the morphological variant possessing parallel arrangement of adjacent polymer chains, has garnered significant attention.[8] This is due to the more simple extraction of β-chitin from squid waste compared to that of α-chitin from crustaceans. Extraction of β-chitin is less resource-intensive due to squid pens being almost entirely β-chitin and proteins at 49.0% and 46.23%, respectively.[9] Moreover, β-chitin is more soluble and reactive than α-chitin, resulting in more efficient deacetylation.[8] However, the progression of chitosan towards utilization in commercial applications has been hindered by low mechanical strength, substantial cost, inadequate chemical stability in acidic media and limited access to binding sites.[10]

The preparation of spherical hydrogel beads from chitosan is a common modification for increasing porosity, surface area and access to internal binding sites.[10, 11] Spherical beads also address the operational limitations associated with powdered or non-structured adsorbents. Additionally, their favourable hydrodynamic behaviour and regular packing confer immense amenability to scale-up under low-pressure conditions without requiring microstructure optimisation, a critical consideration for competing technologies such as two-dimensional material-based (2DM-based) adsorbents.[6, 12]

Chemical crosslinking is the primary strategy for enhancing the stability of chitosan in acidic media. Polymeric networks, with enhanced acidic resistance, are prepared by exploiting the ability of bifunctional crosslinkers to covalently bridge chitosan chains at amine or hydroxyl sites.[8] The preservation of hydrogel structure in acidic media allows for regeneration. However, most crosslinkers are toxic and impart impaired mass transfer as well as brittleness.[10] The affinity of crosslinkers towards amine groups is an additional challenge, resulting in reduced negative surface charge and adsorption capacity. Currently the most reliable and utilized crosslinker is glutaraldehyde, which targets amine sites by imine (Schiff) bond formation.[8]

Ionic liquids (ILs) are compounds, comprised of anions and cations, with melting points not exceeding 100 °C. IL treatment or solubilization is a novel strategy for functionalizing chitosan. This method functions by reducing the crystallinity of chitosan through the rearrangement of chitosan's linear chains.[11, 13] The disruption of inter- and intra-molecular bonds in the amorphous and crystalline regions of chitosan occurs due to the anions of ILs possessing high hydrogen bond accepting abilities, which effectively enable the formation of hydrogen bonds with amine and hydroxyl groups.[14] The merit of IL solubilization as a novel synthesis strategy is supported by the limited uptake of metal ions by chitosan's crystalline planes, with chelation occurring exclusively on the amorphous regions.[15]

IL treatment is operationally simple. It resembles the phase separation method for bead preparation using dilute organic acids. The key difference is regeneration in ethanol or water via an antisolvent mechanism rather than neutralization in alkaline media. [13, 16] This is advantageous as it enables solvent

recycling. IL systems also benefit from good thermal stability, low vapour pressure and cosolvent compatibility.[14]

1-Butyl-3-methylimidazolium acetate ([BMIM][OAc]) is the IL reported to have the highest solvating ability for chitosan with a maximum loading capacity of 8.40% at 100 °C.[14] Additionally, the FT-IR spectrum of chitosan regenerated from [BMIM][OAc] is not indicative of side reactions or the production of ammonium salts, with the primary structure remaining unaltered. However, [BMIM][OAc] is very viscous with dimethyl sulfoxide commonly used as a cosolvent to facilitate extrusion.[16] Lastly, like other ILs, [BMIM][OAc] has been reported in previous work to impart poor mechanical properties on regenerated chitosan beads.[17]

Interpenetrative blending facilitates augmenting chitosan's mechanical strength beyond recasting and has been coupled with IL solubilization to compensate for enhanced brittleness. Interpenetrated polymer networks (IPNs) are comprised of two or more polymers, which have undergone molecular interlacing through diffusion prior to being chemically crosslinked.[18] IPN formulations are noteworthy for their idiosyncratic properties, which can be tuned by altering the co-polymer dosage. Hybrid chitosan-based materials have been reported with enhanced chemical stability, mechanical properties and adsorption capacities.[8] The latter is influenced by the functional groups on the blend polymer(s), with lower pKa values conferring higher negative surface charge.[8] Polysaccharides and proteins are promising blend polymers due to their hydroxyl, sulfhydryl, amine and carboxyl content.

Squid pen (SP) protein, extracted alongside β-chitin from squid gladii (or pens), is postulated to have a high diversity and density of functional groups. The mechanical strength of squid gladii provides motivation for suitability as a co-polymer on the basis that β-chitosan and SP protein hybrid materials can be reverse-engineered to have similar properties. Furthermore, SP protein is an underutilized byproduct of β-chitosan production. As such, its incorporation affords a valuable opportunity to optimize the β-chitosan value chain while subsidizing the cost of a hybrid biosorbent. Partially substituting β-chitosan with SP protein, a starting material, also reduces the environmental footprint of a hybrid biosorbent since chitin deacetylation occurs at 100 – 160 °C over several hours and requires 40 – 50% sodium hydroxide.[8]

This study focused on the synthesis and characterization of highly functionalized and mechanically enhanced hybrid biosorbents from β-chitosan and SP protein by recasting from [BMIM][OAc]. The effect of different SP protein content was studied. The influence of solution pH, agitation period and initial solution concentration on the adsorption of Cu^{2+} and Zn^{2+} by the biosorbents was investigated.

Experimental

Chemicals and Materials

β-chitosan (~580,000 Da) was purchased from Glentham Life Sciences. The degree of deacetylation was 92% as determined by nuclear magnetic resonance (NMR) using a JNM-ECZL 400S spectrometer (JEOL). Sieved squid pen was sourced locally and determined to have a moisture content of 5% after overnight drying at 105 °C. Sodium hydroxide pellets (NaOH, 98.8%) and absolute ethanol (≥96%) were sourced from VWR Chemicals. Deionized (DI) water (≥18 MΩ) was obtained from a Centra R200 (ELGA LabWater). Hydrochloric acid (HCl, ~37%) and nitric acid (HNO_3, ~67-69%) of TraceMetal™ designation were obtained from Fisher Scientific. 1-Butyl-3-methylimidazolium acetate ([BMIM][OAc]) was sourced from Proionic, with a moisture content of 1.75% as determined on a Karl Fischer C20 Coulometer (Mettler Toledo). Glutaraldehyde solution (~50%), dimethyl sulfoxide (DMSO, analytical grade, ≥99.7%), zinc nitrate hexahydrate ($Zn(NO_3)_2 \cdot 6H_2O$, analytical grade, ≥99.0%), and copper (II) sulphate pentahydrate ($CuSO_4 \cdot 5H_2O$, analytical grade, ≥99.0%) were sourced from Sigma-Aldrich. All chemicals were used without modification and stored as recommended.

Squid pen protein extraction

A slurry comprised of 5% squid pen (dry mass) was prepared by the addition of a suitable volume of 0.5 M NaOH solution. The slurry was stirred at 400 rpm and ambient temperature for 3 hours, then vacuum filtered. Isoelectric precipitation (pH 3.5) was performed on the filtrate by the dropwise addition of 3M HCl solution. A Jenway 3510 pH Meter (Cole Parmar) was used for all pH-related measurements. The precipitated protein was centrifuged at 3600 rpm for 20 minutes using a VWR Mega Star 3.0 (Avantor). The supernatant was discarded while the protein was washed with DI water 4 times. The washed protein was immersed in liquid nitrogen and freeze dried for 48 hours on a Freezone^6 (Labconco).

Hydrogel bead preparation

Three distinct types of chitosan-SP protein hydrogel beads were studied. These were designated as CH, CH-SQ-25 and CH-SQ-50, with β-chitosan contents of 100%, 75% and 50%, respectively. The remainder of their content being SP protein.

A batch-equivalent of casting solution was prepared from a solvent system comprised of 12 g [BMIM][OAc] and 12 g DMSO, to which β-chitosan and SP protein were added for a total solid loading of 0.6 g (5% IL mass). The proportion of the co-polymers was dependent on the bead type as previously described. The dissolution of the dispersed polymers was achieved through continuous stirring at 400 rpm and 100 °C for 20 hours. Each batch of casting solution was manually extruded into 250 ml of absolute ethanol using an 18-g needle (ID 0.838 mm) paired alongside a 3 ml syringe. During extrusion, the casting solutions were maintained at 100 °C to reduce viscosity and the 18-g needle was replaced upon clogging. The regenerated hydrogel beads were left to cure for 20 hours in absolute ethanol under gentle stirring at 100 rpm. The cured beads were removed from the ethanol-IL mixture by filtration through a Büchner funnel. The filtrate was discarded. However, the [BMIM][OAc]:DMSO = 1:1 solvent system was recoverable by rotary evaporation. The recovered beads were washed 3 times. This entailed adding the beads to 250 ml of DI water and stirring at 100 rpm for an hour prior to filtration. The washed beads were added to 100 ml of 0.25% glutaraldehyde solution and crosslinked for 20 hours under gentle stirring at 100 rpm. A similar recovery and washing scheme as detailed after curing was observed. The crosslinked beads were then immersed in liquid nitrogen and freeze dried for 48 hours using a Freezone^6.

Microscopy

The hydrogel beads were observed with a Leica DM2500 (Leica). Their internal network was analysed by pressing a sample bead between glass slides under 4X magnification with light directed from above.

Fourier Transform Infrared Spectroscopy (FT-IR)

The FT-IR spectra of β-chitosan, SP protein, and the hydrogel beads were recorded on an Agilent Cary 630 (Agilent) equipped with a Diamond-ATR sampling module obtained from the same manufacturer. The hydrogel beads were pulverized for analysis but otherwise remained unmodified. The spectral acquisition was performed over the range of 4000 – 500 cm^{-1} with 32 sample scans at room temperature.

Zeta Potential

The mean zeta potentials of β-chitosan and SP protein were determined using a Litesizer 500 (Anton Paar). The polymers were suspended in DI water and loaded into omega cuvettes, from the same manufacturer, for analysis. All measurements were performed at room temperature.

Preparation of synthetic wastewater

Cu^{2+} and Zn^{2+} solutions with concentrations of 50, 100, 150, 200 and 250 ppm were prepared by dissolving the appropriate amounts of either $CuSO_4 \cdot 5H_2O$ or $Zn(NO_3)_2 \cdot 6H_2O$ in DI water.

Adsorption Experiments

The adsorption characteristics of the hydrogel bead types were assessed by batch studies involving the addition of hydrated beads to either copper or zinc wastewater in 50 ml centrifuge tubes. The agitation speed, solution volume, biosorbent mass and metal ion concentration were dependent on the specific experiment as described in the following sections. Equipment-wise, all instances of centrifugation and pH measurements were performed on the aforementioned equipment while agitation was provided using a Multi Reax Orbital Shaker (Heidolph).

The metal ion concentration, C_t, in the treated wastewater samples was determined twice by inductively coupled plasma mass spectroscopy on an Agilent 7900 ICP-MS (Agilent). A dilution matrix comprised of 1% HCl and 2% HNO_3 was utilized alongside commercial calibration standards. The removal efficiency, R_e, of heavy metal ions was calculated according to the following equation:

$$R_e = \frac{C_i - C_t}{C_i} \times 100 \quad (1)$$

where C_i is the heavy metal ion concentration (ppm) before treatment.

The amount of heavy metal ions adsorbed per dry mass of biosorbent or adsorption capacity, q_t, in mg g^{-1} was calculated according to the following equation:

$$q_t = \frac{C_i - C_t}{m_{dry}} \times V \quad (2)$$

where V is the volume of the heavy metal ion solution (L) and m_{dry} is the dry mass of the biosorbent (g).

Initial pH studies

Experiments relating to Cu^{2+} were performed within the pH range of 2 – 5. Meanwhile, experiments with Zn^{2+} used the pH range of 3 – 6. These pH ranges were suitable to prevent the precipitation of the insoluble hydroxide complexes of the respective metal ions.[19, 20] A slightly modified protocol proposed by Sutirman et. al. was used for the experiments.[21] For each batch study, 0.025 g of each bead type were hydrated in 20 ml of DI water. The hydrated beads were filtered to remove excess water prior to being transferred into 12 ml of 100 ppm Cu^{2+} or Zn^{2+} solutions at the various integer pH values within the ranges. An initial pH method was used with the pH value of the solutions not being adjusted during the adsorption period. For consistency, the initial adjustments to the pH value were done on 100 ml aliquots of 100 ppm Cu^{2+} or Zn^{2+} solution from the same stock solution. Solutions of 0.1 M NaOH and 0.1 M HCl were used to perform the initial adjustments. The immersed beads were agitated/treated at 800 rpm for an hour. The treated wastewater solutions were centrifuged at 4000 rpm for 3 minutes, with acceleration and braking levels set at 9. The supernatants were filtered through a 0.2 μm filter for analysis.

Kinetic studies

CH-SQ-25 beads, the hybrid beads with the highest removal efficiency in the pH studies, were utilized to obtain kinetic data. Similarly, the optimum conditions from the previous section were used to maximize adsorption. The experiments were slightly modified from the pH studies. The scale was increased four-fold to enable repeated sampling without vastly altering the solution volume. Firstly, 0.1 g of CH-SQ-25 beads were hydrated for 24 hours in 40 ml of DI water. The hydrated beads were filtered to remove excess water and transferred to 48 ml of 100 ppm Cu^{2+} or Zn^{2+} solution at the optimum pH value (Cu^{2+} pH 5, Zn^{2+} pH 6). The immersed beads were agitate at 1200 rpm. The higher speed reflected the larger scale. A 1 ml syringe was utilized for sample withdrawal at the following time intervals: 30 minutes, 60 minutes, 90 minutes, 3 hours, 6 hours, and 24 hours. The samples were filtered through a 0.2 μm filter for analysis.

Equilibrium studies

CH-SQ-25 beads and optimum conditions were used as stated in the previous section. These experiments closely resembled those performed by Sutirman et. al.[21] The main difference was the selection of 50 – 250 ppm as the concentration range based on studies conducted by Wittmer et. al.[16] For each study, 0.025 g of CH-SQ-25 beads were hydrated for 24 hours in 20 ml of DI water. The hydrated beads were filtered to remove excess water and transferred to 12 ml of Cu^{2+} or Zn^{2+} solution at the various concentration and optimum pH value (Cu^{2+} pH 5, Zn^{2+} pH 6). The beads were agitated at 900 rpm for 24 hours. The slightly more intense agitation speed was selected to prevent settling during the longer period. After 24 hours, the treated wastewater solutions were centrifuged at 4000 rpm for 3 minutes, with acceleration and braking levels set at 9. The supernatant was filtered through a 0.2 μm filter for analysis.

Results and discussion

Physical Characterization

The beads obtained by recasting from [BMIM][OAc] exhibited less-defined geometries with increasing SP protein content. CH beads were spherical, whereas CH-SQ-25 and CH-SQ-50 beads were ellipsoidal with visible voidage. These findings were supported by size measurements, which revealed an increase in length and decrease in width at higher SP protein content (**Figure 1**). Furthermore, all bead types displayed brittleness, with CH-SQ-50 beads being the most fragile and pulverizing when gently pressed.

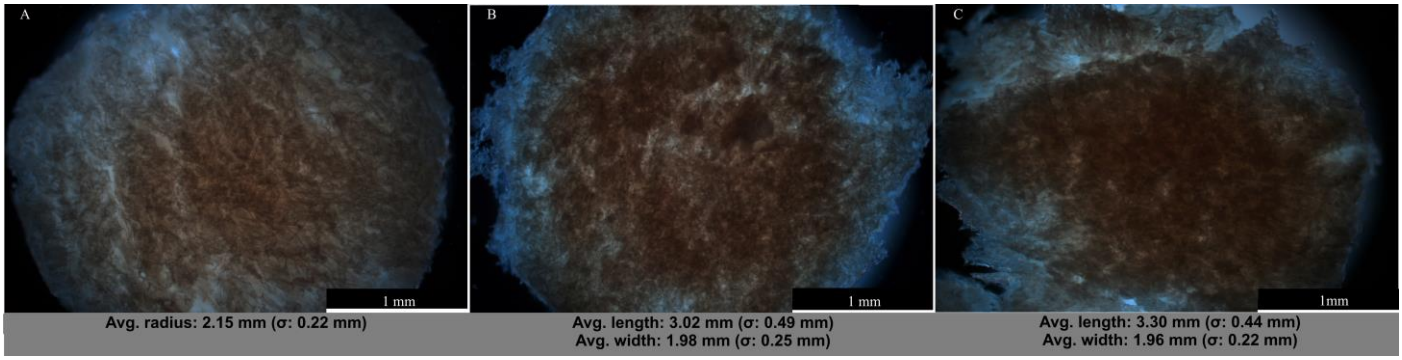

Figure 1: Average size measurements and optical microscopy at 4X magnification of internal network of (A) CH beads, (B) CH-SQ-25 beads, (C) CH-SQ-50 beads

Optical microscopy was employed to examine the internal network of the beads (**Figure 1**). CH beads revealed a dense network of β-chitosan fibres characterized by homogenous interweaving and very rough morphology. For CH-SQ-25 and CH-SQ-50 beads, SP protein content resulted in heterogeneity as evidenced by the presence of sections of poorly interwoven fibres. Additionally, CH-SQ-50 beads revealed dense clumps with very little or no discernible organization.

The non-uniformity of CH-SQ-25 and CH-SQ-50 beads may indicate poor interlacing among the functional groups on SP protein and β-chitosan. However, methodological factors must also be considered. For example, the total solid loading was maintained constant, which overlooked β-chitosan having a larger molecular weight than SP protein. Consequentially, the casting solutions for the different bead types had pronounced variations in viscosity, an extrusion parameter which influences porosity, surface area and shape.[16] In practice, extrusion from an 18-g needle may have been adequate for the highly viscous casting solution of CH beads but unsuitable for the notably less viscous casting solutions of CH-SQ-25 and CH-SQ-50 beads.

Similarly, SP protein was determined to enhance brittleness. However, the brittleness of the CH beads was indicative of other contributors. For example, crosslinking has been associated with enhanced fragility. This was evident in earlier experiments, such that the glutaraldehyde concentration was maintained relatively low (0.25%) as a deterrent. Therefore, IL treatment using [BMIM][OAc] must have also imparted poor mechanical properties. This was consistent with observations for chitosan regeneration from [BMIM][Cl], as reported by Sun et. al.[13]

Fourier Transform Infrared (FT-IR) Spectra

FT-IR spectral analysis of β-chitosan and SP protein elucidated the chemical and structural derivatives present on the polymer chains (**Figure 2).** The spectrum for β-chitosan was consistent with previous studies. The band at 3303 cm^{-1} related to overlap between N—H and O—H stretching vibrations.[21] The band at 2864 cm^{-1} was allocated to symmetric and asymmetric C—H and CH_2 stretching.[14, 21] The bands at 1645 and 1589 cm^{-1} were due to C=O stretching (Amide I) of the residual acetamido groups and N—H deformation vibrations of NH_2 groups (Amide II), respectively.[21] The band at 1422 cm^{-1} was attributed to N—H deformation vibrations of NH_2 while the band at 1319 cm^{-1} related to C—N stretching vibrations. The band at 1373 cm^{-1} was assigned to C—H deformation.[22] The bands at 1153 and 890 cm^{-1} were assigned to C—H stretching.[23] Lastly, the prominent band at 1023 cm^{-1} was characteristic of the C—O stretching vibrations of the C—O—C bridge.[21, 22] For SP protein, defining bands relating to secondary structure were

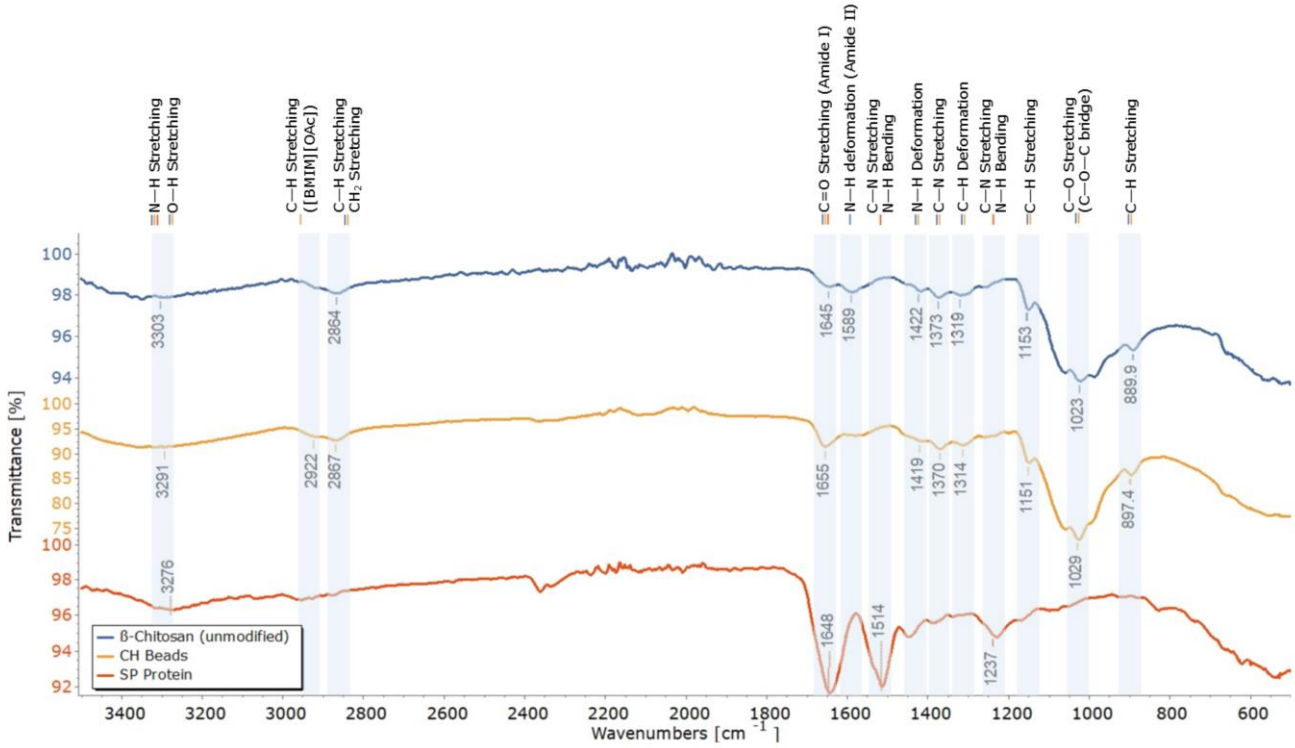

Figure 2: FT-IR spectra of unmodified β-chitosan, CH beads (100% β-chitosan) regenerated from [BMIM][OAc] and SP protein

observed. The band at 1648 cm^{-1} was assigned to amide I vibrations arising from C=O stretching while the band at 1514 cm^{-1} was the combination of C—N stretching and N—H bending.[24] The amide III band at 1237 cm^{-1} related to C—N stretching and N—H bending. The band at 3276 cm^{-1} indicated O—H stretching.

The spectra of β-chitosan and CH beads were compared to assess the effectiveness of IL treatment in [BMIM][OAc] as a functionalization strategy (**Figure 2**) Both spectra exhibited the same bands, with negligible shifting. Notably, the bands at 3291 and 1029 cm^{-1} were considerably more intense for CH beads. This corresponded with the enhanced inter- and intramolecular interactions arising from the rearrangement of β-chitosan's crystalline planes by the acetate anions.[22] Additionally, the characteristic bands related to ammonium did not decrease in intensity as expected after crosslinking. For reference, decreases in band intensity at 3291, 1655, 1419, 1314 and 1151 cm^{-1} have been previously reported from crosslinking with glutaraldehyde.[21, 25] The only indication of crosslinking was the disappearance of the band at 1589 cm^{-1} related to N—H bending of NH_2 groups. Lastly, a band indicative of aliphatic C—H stretching vibrations of methyl groups on the [BMIM] cation appeared at 2922 cm^{-1} on the CH beads' spectrum serving as the only evidence of IL treatment and suggesting inefficient curing or washing stages.[26]

Figure 3A illustrates the spectra for the various beads types. Close similarity between the spectra was noted. Notably, no contribution from SP protein was discerned on the spectra for CH-SQ-25 and CH-SQ-50 beads. Additionally, the intensity of the bands at 3291, 2867, 1419, 1370, 1314 and 1029 cm^{-1} decreased as the SP protein content increased, indicating that the SP protein did not enhance the functional group density on the biosorbents with β-chitosan being the primary contributor.

The 1700 – 1450 cm^{-1} spectral range offered insight in the absence of discernible bands related to SP protein on the FT-IR spectra for CH-SQ-25 and CH-SQ-50 beads. From **Figure 3B**, it was observed that amide I vibrations were shared by SP protein and CH beads (regenerated β-chitosan) at 1655 and 1648 cm^{-1}, respectively. It is probable that hydrogen bonding among the polymers resulted in the bands for CH beads and SP protein shifting slightly and merging at 1653 cm^{-1} on the spectra

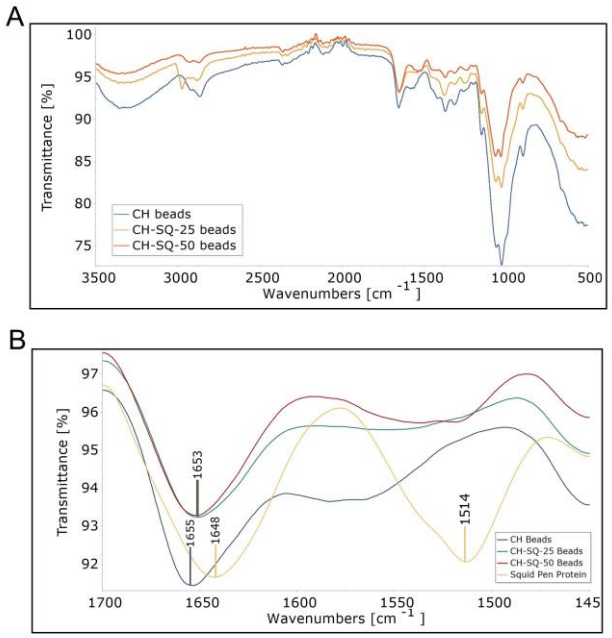

Figure 3: FT-IR Spectra of CH, CH-SQ-25 and CH-SQ-50 beads showing the effect of SP protein content over (A) 3500 – 500 cm^{-1} spectral range (B) 1700 – 1450 cm^{-1} spectral range with inclusion of SP protein spectrum for comparison

of CH-SQ-25 and CH-SQ-50 beads. As for the amide II band present at 1514 cm^{-1} on the spectrum for SP protein, the absence from the spectra of CH-SQ-25 and CH-SQ-50 beads has been attributed to glutaraldehyde crosslinking.

Influence of pH

The effect of solution pH on the adsorption of heavy metal ions by the different bead types was investigated to understand the influence of surface charge. The determination of an optimum pH value for the subsequent studies was an added objective.

The efficiency of Cu^{2+} removal from a 100-ppm solution by the different beads types was recorded for different pH values after an hour of treatment (**Figure 4A**). All bead types exhibited a similar pH dependence, with Cu^{2+} uptake increasing sharply over the pH range of 2 – 3, after which improvements became gradual. Importantly, statistical differences were not noted at higher pH levels (4 – 5). An optimum pH value of 5 was noted.

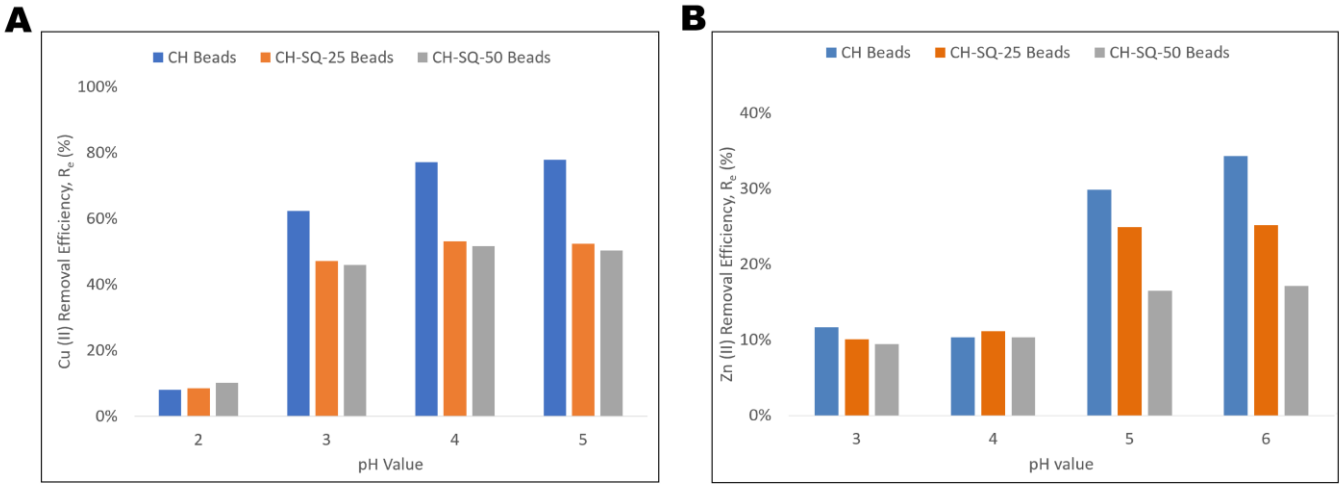

Figure 4: The effect of solution pH on the removal efficiencies achieved by CH-SQ-25, and CH-SQ-50 beads from 100 ppm heavy metal ion solutions

The removal of Zn^{2+} by the beads was investigated under identical conditions (**Figure 4B**). All bead types showcased a similar pH dependence with uptake being relatively low within the pH range of 3 – 4 before sharply increasing in the range of 4 – 5. For higher pH values (5 – 6), the removal efficiency of Zn^{2+} only slightly increased. The results suggested an optimum pH of 6.

The increase in the removal efficiencies of Cu^{2+} and Zn^{2+} at the higher pH values suggests that the adsorption of heavy metal ions was regulated by the surface charge of the beads, particularly from the protonation of non-crosslinked amine groups.[11] Protonation entails electrostatic repulsion of heavy metal cations and unfavourable adsorption due to competitive occupation of active sites by protons.[11, 19] The opposite effect at high pH values accounts for more favourable adsorption. This was not observed experimentally possibly due to reduced sensitivity at higher pH levels. However, it must be noted that the heavy metal ion solutions were unbuffered. Moreover, no adjustments were performed during the agitation period.

Under identical conditions, all bead types exhibited a lower affinity for Zn^{2+}. Previous studies have reported similar results for Zn^{2+} and Cu^{2+} for both single-ion and competitive batch adsorption studies.[27] The consensus is that the adsorption of bivalent heavy metal ions onto chitosan is governed by the Irving-William series, which describes the stability of bivalent transition metal complexes, with Cu^{2+} being the most stable.[28]

Regarding bead type, higher SP protein content negatively affected the removal efficiencies of Zn^{2+} (**Figure 4B**). For Cu^{2+}, CH beads had a greater affinity. However, the difference in uptake by CH-SQ-25 and CH-SQ-50 beads was small (**Figure 4A**). The lack of a similar trend for Zn^{2+} may be attributed to a lower affinity for chelation with chitosan. In general, the results suggested that SP protein was not suitable as a functional agent for heavy metal ion adsorption. This was consistent with the FT-IR spectra for CH-SQ-25 and CH-SQ-50 beads, which showed a decrease in functionalization at higher SP protein content. The mean zeta potentials, under neutral condition, for SP Protein and β-chitosan of 26.6 mV and 11.6 mV, respectively, offered a supplementary explanation with higher cationic surface charge on SP protein being supportive of greater resistance for the adsorption of Cu^{2+} and Zn^{2+}. Notably, inherently higher cationic surface charge of SP protein may enhance interactions with heavy metal ions that exist as anionic coordination compounds (e.g. $HCrO_4^-$ and $PdCl_4^{2-}$), which did not form part of the study.[6]

Lastly, desorption studies were not performed. However, CH and CH-SQ-25 beads maintained their mechanical integrity after agitation and recovery. This demonstrated great potential, except for slight vulnerability to acidic conditions as observed with partial dissolution at pH 2 for the Cu^{2+} studies. For CH-SQ-50 beads, breakage was observed, but the extent was difficult to assess due to significant variation in bead geometry. Overall, the findings do not discredit SP protein as a filler co-polymer, since it is directly derived from the same biomass as β-chitosan

Kinetic studies

Kinetic studies offered insight into the mechanism behind heavy metal ion uptake by CH-SQ-25 beads. The pseudo-first-order (PFO) and pseudo-second-order (PSO) models were used. These studies also investigated the suitability of a 24-hour treatment period with regards to approaching equilibrium.

Figure 5A illustrates the time-course adsorption of Cu^{2+} by CH-SQ-25 beads from a 100-ppm solution. Equilibrium was gradually approached over the 24-hour treatment period at an adsorption capacity of 40.1 mg g^{-1}. Notably, adsorption was initially rapid as evidenced by the adsorption capacity after 3 hours being 32.8 mg g^{-1} or 83% of the equilibrium value.

The kinetics for Zn^{2+} removal were also studied (**Figure 5B**). The equilibrium adsorption capacity was 8.3 mg g^{-1} after 24 hours of treatment. Remarkably, this was almost achieved after only 6 hours, at a corresponding adsorption capacity of 8.1 mg g^{-1}. The remainder of the initial treatment period was equally rapid with 6.3 mg g^{-1}, or 76% of the equilibrium value having been adsorbed after 3 hours. Notably, the time-course removal efficiency after 1 hour was 9% as opposed to 25% from the pH studies, which suggests batch variation in the synthesis of the same bead type or scale-up limitations. The discrepancy was not noted for Cu^{2+}, which may indicate that the lower affinity for Zn^{2+} may have been a factor.

The parameters for the PFO and PSO kinetic models are given on **Table 1**. Notably, the correlation coefficients, R^2, of the PSO model were >0.9990 compared to >0.9649 for the PFO model. Furthermore, the estimated equilibrium capacities from the PSO model agreed with the experimentally obtained values for both Cu^{2+} and Zn^{2+}. With regards to the PFO model, the experimental and theoretical values differed by more than 10%. Plotting the PFO and PSO models with the obtained parameters (**Figure 5**) visualized the more precise fit provided by the latter model over the entire time domain. Therefore, the PSO model

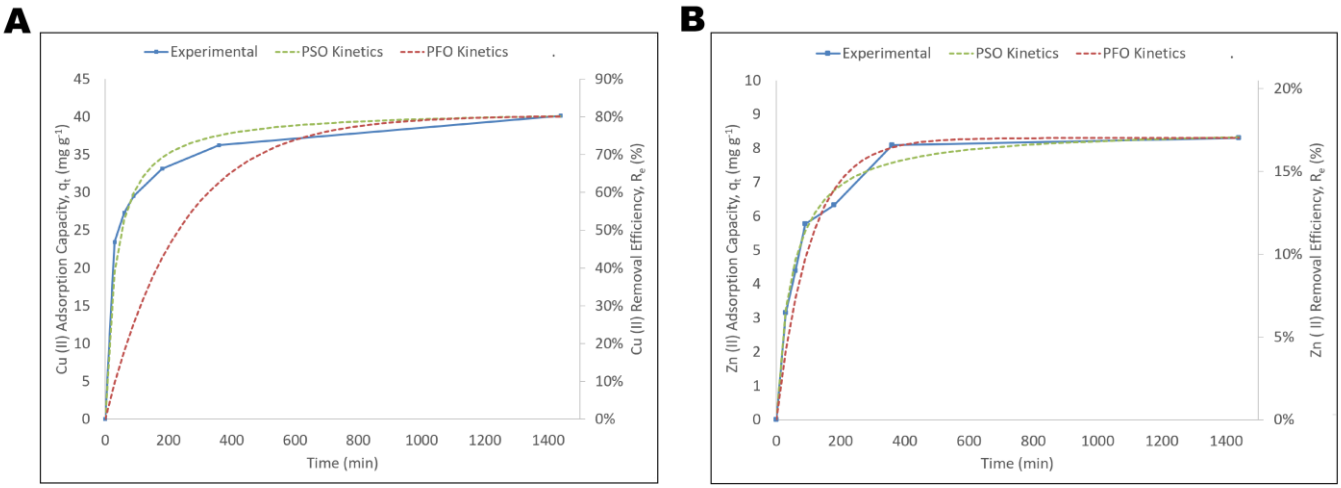

Figure 5: Equilibrium isotherms for 24-hour treatment by CH-S-Q25 beads of heavy metal ion solutions

was accepted to describe the adsorption of both Cu^{2+} and Zn^{2+}. This suggested that the mechanism or rate-limiting step for adsorption was chemisorption or complexation based on the sharing or exchange of electrons between the heavy metal ions and the adsorbent functional groups.[11, 21]

Equilibrium studies

The surface characteristics of CH-SQ-25 beads were elucidated through equilibrium adsorption studies. The Freundlich and Langmuir isotherms were employed to assess the distribution of heavy metal ions between the beads and the solution at equilibrium, with a 24-hour treatment period deemed suitable from kinetic studies. Analysis focused on the saturation of active sites due to excess heavy metal ions (i.e. high concentrations), with the isotherms enabling the determination of maximum adsorption capacities, q_m, for $Cu^{2+}$and Zn^{2+}, for comparison with previous work.

The equilibrium isotherm for Cu^{2+} adsorption by CH-SQ-25 beads was obtained for the concentration range of 50 – 250 ppm (**Figure 6A**). The onset of active site saturation was observed. However, complete saturation was not achieved. Moreover, the Langmuir isotherm offered a better description, with a correlation coefficient, R^2, of 0.9938 compared to 0.9792 for the Freundlich isotherm (**Table 1**).

The effect of initial solution concentration on Zn^{2+} uptake by CH-SQ-25 beads was investigated under identical conditions (**Figure 6B**). Notably, a high degree of linearity suggested that the concentration range was too low to promote saturation of active sites. Additionally, both the Langmuir and Freundlich isotherms were in good accordance with the experimental data, as indicated by correlation coefficients of 0.9980 and 0.9943, respectively (**Table 1**). This is believed to have resulted from Henry's law not being satisfied for Zn^{2+} adsorption over the low concentration range, resulting in the collapse of the Freundlich isotherm.[29] Intuitively, the results suggest that adsorption was limited to monolayer coverage since the concentration range was inadequate to support multilayer coverage. Therefore, the Langmuir isotherm best described the adsorption of Zn^{2+}.

The suitability of the Langmuir isotherm for both Cu^{2+} and Zn^{2+} suggests that adsorption occurs via monolayer coverage of homogeneous active sites, with negligible interactions among the adsorbed heavy metal ions.[11, 21]

Based on the Langmuir isotherm, the CH-SQ-25 beads had a maximum adsorption capacity of 70.2 and 24.0 mg g^{-1} for Cu^{2+} and Zn^{2+}, respectively (**Table 1**). These values confirmed that the concentration range was inadequately low since the studies only achieved adsorption capacities of 65.5 and 12.1 mg g^{-1} for Cu^{2+} and Zn^{2+}, respectively. In fact, only 50% of the maximum adsorption capacity for Zn^{2+} was achieved.

The lower affinity of CH-SQ-25 beads for Zn^{2+} was supported by a lower maximum adsorption capacity compared to the value for Cu^{2+}. This observation was consistent with previous studies. The Langmuir constant, K_L, provided additional evidence of the lower affinity for Zn^{2+} (**Table 1**). In this regard, the much large K_L value for Cu^{2+} (0.0815 L mg^{-1}), compared to the value for Zn^{2+} (0.0046 L mg^{-1}), indicated a much stronger binding affinity. Further elucidation of the lower affinity of CH-SQ-25 beads for Zn^{2+} was provided by the Langmuir equilibrium parameters, R_L, for which lower values within the range of 0 – 1 indicate more favourable adsorption. In this regard, the R_L values for Zn^{2+} exceeded 0.4 over the entire initial concentration range while those for Cu^{2+} were consistently lower than 0.2. Regardless, the adsorption of both heavy metal ions was favourable. Notably, the lower affinity for Zn^{2+} has previously been attributed to the higher stability of Cu^{2+} complexes on the William-Irving series.

Table 1: Parameters for kinetic models and equilibrium isotherms for Cu^{2+} and Zn^{2+} adsorption by CH-SQ-25 beads

Heavy metal ion	Kinetic models[a]					Equilibrium isotherms					
	Experimental	PFO[b]		PSO[b]		Langmuir[b]					Freundlich[b]
	q_e (mg g^{-1})	q_e (mg g^{-1})	R^2	q_e (mg g^{-1})	R^2	q_m (mg g^{-1})	R^2	K_L (L mg^{-1})	R_{L_U}[c]	R_{L_L}[d]	R^2
Cu^{2+}	40.1	16.7	0.9709	41.0	0.9997	70.2	0.9938	0.0815	0.195	0.046	0.9792
Zn^{2+}	8.3	7.1	0.9649	8.61	0.9993	24.0	0.9980	0.0046	0.816	0.471	0.9943

[a] For a solution concentration of 100 ppm [b] Only parameters & correlation coefficients mentioned in the main text are shown. The complete set of parameters are available as supporting information. [c] R_{L_U} is the upper-limit Langmuir equilibrium parameter at 50 ppm [d] R_{L_L} is the lower-limit Langmuir equilibrium parameter at 250 ppm

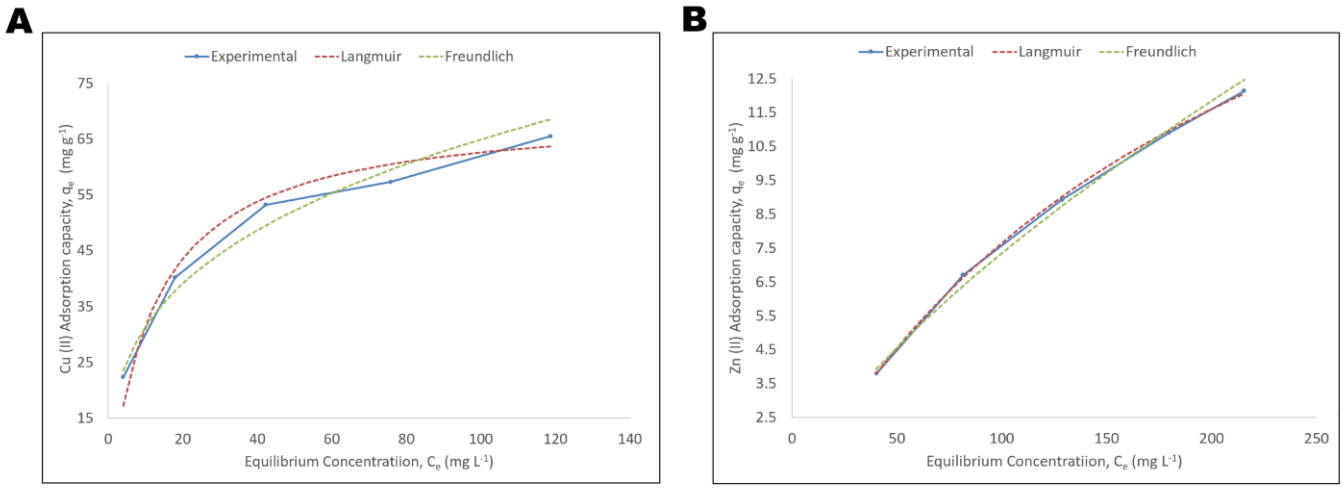

Figure 6: Equilibrium isotherms for 24-hour treatment by CH-SQ-25 beads of heavy metal ion solutions

Lastly, CH-SQ-25 beads were competitive performance compared to other chitosan-based beads reported in literature (**Table 2**). Appreciable improvements for the adsorption of Zn^{2+} and Cu^{2+} compared to other crosslinked hydrogel beads were reported. Only conventional grafting yielded chitosan-based biosorbents possessing maximum adsorption capacities that surpassed those of CH-SQ-25 beads. This highlighted the effectiveness of IL treatment using [BMIM][OAc] as a highly convenient functionalization method, which can compensate for losses in adsorption capacity from crosslinking without requiring the complexity associated with conventional grafting.

Sustainability Metrics

The promotion of green chemistry in the synthesis of chitosan-based adsorbents by recasting from [BMIM][OAc] was assessed. Atom economy and E-factor were employed. The calculations focused solely on the CH bead type due to the certainty of functional groups on β-chitosan with 92% deacetylation and molecular weight of approximately 580 kDa.

Atom economy was evaluated in the context of crosslinking with glutaraldehyde by imine bond formation, involving condensation reactions. A conservative value of 91.61% was obtained for the complete saturation of amine sites. However, this scenario was unlikely due to the participation of free amine sites in the adsorption of heavy metal ions. The actual atom economy has been projected between 91.61 – 100%.

The E-factor considered the recyclability of [BMIM][OAc], DMSO and absolute ethanol, as well as the full recovery of β-chitosan in the CH beads. Losses solely considered the spent glutaraldehyde solution. An optimal estimate of 0.105 was noted for the retention of glutaraldehyde corresponding to complete saturation of amine sites. However, acknowledging the non-crosslinked amine sites, a conservative estimate was obtained under the assumption of no crosslinking and the loss of all glutaraldehyde solution. The actual E-factor has been projected between 0.105 – 0.441.

The preparation of chitosan-based beads by IL treatment in [BMIM][OAc] exhibited excellent atom economy and low E-factor. Furthermore, using SP protein as a co-polymer affords additional merit by decreasing the environmental footprint and overall cost of the biosorbents, given that β-chitosan is much more costly due to the resource intensiveness of its synthesis.

Conclusion

Biosorbent beads for heavy metal ion removal from wastewater were successfully prepared from β-chitosan and SP protein, by regeneration from [BMIM][OAc]. The mechanical, functional and adsorptive properties of the hybrid biosorbents beads were investigated to assess the contributions of SP protein.

Physical characterisation uncovered increased brittleness at higher SP protein content in CH-SQ-25 and CH-SQ-50 beads. Additionally, observable brittleness in CH beads suggested that IL treatment in [BMIM][OAc] contributed to fragility. This served to indicate a need to optimize the composition of the beads and the preparation process, particularly the extrusion procedures, which may have been more suitable for beads with lower SP protein and more viscous casting solutions. Furthermore, BET analysis should be utilized to investigate whether greater non-uniformity in the internal networks of CH-SQ-25 and CH-SQ-50 beads, resulting from SP protein content, may have enhanced the surface area.

FT-IR analysis revealed that IL regeneration enhances the functional group availability on chitosan. However, SP protein was noted to diminish β-chitosan's characteristic bands. Given a relationship between FT-IR intensity and co-polymer dosage, X-ray photoelectron spectroscopy (XPS) may be used for the analysis of specific functional groups, such as N-containing groups. Alternatively, titration may be adopted for quantitative analysis of active functional groups.

Adsorption studies highlighted less efficient heavy metal ion removal at lower pH levels, with adsorption being optimal at pH 5 and 6 for Cu^{2+} and Zn^{2+}, respectively. Concerning SP protein, it was observed that higher contents corresponded to a decrease in the removal efficiency of Cu^{2+} and Zn^{2+}. Additionally, kinetic studies with CH-SQ-25 beads showed rapid adsorption of Cu^{2+} and Zn^{2+}, following pseudo-second-order kinetics, which is indicative of chemisorption. Meanwhile, equilibrium studies based on the Langmuir isotherm indicated that CH-SQ-25 beads have higher maximum adsorption capacities for Cu^{2+} and Zn^{2+} than similar hydrogel beads reported in literature. Notably, further investigations should be conducted using other heavy metals ions, particularly anionic coordination compounds, to elucidate the influence of the higher cationic surface charge of SP protein on the removal of multifarious heavy metal ions.

The inclusion of SP protein did not improve the heavy metal adsorption capability of chitosan. However, its inclusion as a cost-reducing filler may be suggested considering IL treatment's potential for effective β-chitosan functionalization

Table 2: Preparation methodology and maximum adsorption capacity (mg g^{-1}) of chitosan biosorbent hydrogel beads from literature

Modification type	Specific preparation method	Heavy metal ions		Authors
		Cu^{2+}	Zn^{2+}	
Crosslinking	Sodium polyphosphate	26.06	-	Wan Ngah & Fatinathan[29]
Crosslinking	Glutaraldehyde	59.67	-	Wan Ngah et. al.[30]
Crosslinking	Epichlorohydrin	35.46	10.21	Chen et. al.[31]
IL treatment, IPN	Chitosan-cellulose (1:2) from [EMIM][Cl]	36.03	3.45	Matsumoto et. al.[27]
IL treatment, IPN	Chitosan-cellulose (1:2) from [BMIM][Cl]	26.46	19.81	Sun et. al.[13]
IL treatment, IPN	Chitosan-cellulose (1:3) from [BMIM][OAc]	26.70	-	Wittmar et. al.[16]
IL treatment, IPN	Chitosan-cellulose (1:3) from [EMIM][OAc]	15.80	-	
Grafting	Enediaminetetraacetic acid (EDTA)	31.64	24.27	Karimi et. al.[32]
Grafting	Polyaniline	83.3	-	Igberase et. al.[11]
Crosslinking, grafting	Methacrylamide	140.9	-	Sutirman et. al.[21]
Crosslinking, grafting	4-Aminobenzoic acid, epichlorohydrin	140.5	130.6	Igberase et. al.[33]
Crosslinking, grafting	8-Hydroxyquinoline	52.9	8.20	Barros et. al.[34]
IL treatment, IPN, Crosslinking	**CH-SQ-25 Beads**	**70.2**	**24.0**	**This study**

Data availability

The data supporting this article have been included as part of the Supplementary Information.

Conflicts of interest

There are no conflicts to declare

Acknowledgements

The research reported here was funded by the Commonwealth Scholarship Commission and the Foreign, Commonwealth and Development Office in the UK. I am grateful for their support. All views expressed here are those of the author(s) not the funding body. PYSN and JH are also grateful to the UKRI for support through the Supergen Bioenergy Impact Hub 2023 (EP/Y016300/1).

References

1. S. K. Gunatilake, *Journal of Multidisciplinary Engineering Science Studies*, 2015, **1**, 12-18.
2. R. Verma and P. Dwivedi, *Recent Res. Sci. Technol.*, 2013, **5**, 98-99.
3. S. Sarode, P. Upadhyay, M. A. Khosa, T. Mak, A. Shakir, S. Song and A. Ullah, *Int. J. Biol. Macromol.*, 2019, **121**, 1086-1100.
4. Renu, M. Agarwal and K. Singh, *J. Water Reuse Desalin.*, 2017, **7**, 387-419.
5. N. A. A. Qasem, R. H. Mohammed and D. U. Lawal, *npj Clean Water*, 2021, **4**.
6. X. Xie, C. Chen, N. Zhang, Z.-R. Tang, J. Jiang and Y.-J. Xu, *Nat. Sustain.*, 2019, **2**, 856-864.
7. K. H. Carrasco, E. G. Höfgen, D. Brunner, K. B. L. Borchert, B. Reis, C. Steinbach, M. Mayer, S. Schwarz, K. Glas and D. Schwarz, *Polysaccharides*, 2022, **3**, 356-379.
8. L. A. M. Van Den Broek and C. G. Boeriu, *Chitin and Chitosan: Properties and Applications*, John Wiley & Sons, Hoboken, NJ, 2020.
9. E. S. Abdou, K. S. A. Nagy and M. Z. Elsabee, *Bioresour. Technol.*, 2008, **99**, 1359-1367.
10. B. Qu and Y. Luo, *Int. J. Biol. Macromol.*, 2020, **152**, 437-448.
11. E. Igberase, P. Osifo and A. Ofomaja, *J. Environ. Chem. Eng.*, 2014, **2**, 362-369.
12. D. Kong, S. R. Foley and L. D. Wilson, *Molecules*, 2022, **27**.
13. X. Sun, B. Peng, Y. Ji, J. Chen and D. Li, *AIchE J.*, 2009, **55**, 2062-2069.
14. Q. Chen, A. Xu, Z. Li, J. Wang and S. Zhang, *Green Chem.*, 2011, **13**, 3446-3452.
15. S.-T. Lee, F.-L. Mi, Y.-J. Shen and S.-S. Shyu, *Polymer*, 2001, **2001**, 1879-1892.
16. A. S. M. Wittmar, H. Bohler, A. L. Kayali and M. Ulbricht, *Cellulose (Dordrecht, Neth.)*, 2020, **27**, 5689-5705.
17. I. O. Saheed and F. B. M. Suah, *Int. J. Biol. Macromol.*, 2023, **241**.
18. E. S. Dragan, *Chem. Eng. J. (Amsterdam, Neth.)*, 2014, **243**, 572-590.
19. Z. A. Sutirman, M. M. Sanagi, K. J. Abd Karim, W. A. Wan Ibrahim and B. H. Jume, *Int. J. Biol. Macromol.*, 2018, **116**, 255-263.
20. G. Karthikeyan, K. Anbalagan and N. Muthulakshmi Andal, *J. Chem. Sci. (Berlin, Ger.)*, 2004, **116**, 119-127.
21. Z. A. Sutirman, M. M. Sanagi, K. J. Abd Karim and W. A. Wan Ibrahim, *Carbohydr. Polym.*, 2016, **151**, 1091-1099.
22. S. Islam, L. Arnold and R. Padhye, *BioMed Res. Int.*, 2015, **2015**.
23. N. Li and R. Bai, *Ind. Eng. Chem. Res.*, 2005, **44**, 6692-6700.
24. A. Barth, *Biochim. Biophys. Acta, Bioenerg.*, 2007, **1767**, 1073-1101.
25. W. S. Wan Ngah and S. Fatinathan, *Chem. Eng. J. (Amsterdam, Neth.)*, 2008, **143**, 62-67.
26. S. A. Dharaskar, M. N. Varma, D. Z. Shende, C. Kyoo Yoo and K. L. Wasewar, *Sci. World. J.*, 2013, **2013**.
27. M. Matsumoto, S. Ishikawa and T. Kamigaki, *Prog. Chem. Appl. Chitin Its Deriv*, 2019, **24**, 145-150.
28. A. Miličević, G. Branica and N. Raos, *Molecules*, 2011, **16**, 1103-1112.
29. W. S. Wan Ngah and S. Fatinathan, *J. Environ. Manage.*, 2010, **91**, 958-969.
30. W. S. Wan Ngah, C. S. Endud and R. Mayanar, *React. Funct. Polym*, 2002, **50**, 181-190.
31. A.-H. Chen, S.-C. Liu, C.-Y. Chen and C.-Y. Chen, *J. Hazard. Mater.*, 2008, **154**, 184-191.
32. F. Karimi, A. Ayati, B. Tanhaei, A. L. Sanati, S. Afshar, A. Kardan, Z. Dabirifar and C. Karaman, *Environ. Res.*, 2022, **203**.
33. E. Igberase, A. Ofomaja and P. O. Osifo, *Int. J. Biol. Macromol.*, 2019, **123**, 664-676.
34. F. C. F. Barros, S. F. W, R. M. Cavalcante, T. V. Carvalho, F. S. Dias, D. C. Queiroz, L. C. G. Vasconcellos and R. F. Nascimento, *Removal of Copper, Nickel and Zinc Ions from Aqueous Solution by Chitosan-8-Hydroxyquinoline Beads*, 2008, **36**, 292-298.